Chaos and regularity in the spectra of the low-lying dipole excitations of ^{50,52,54}Cr

B. Dietz,[1,*] B. A. Brown,[2,†] U. Gayer,[3] N. Pietralla,[3,‡] V. Yu. Ponomarev,[3,§] A. Richter,[3,‖] P. C. Ries,[3] and V. Werner[3]

[1]*School of Physical Science and Technology, and Key Laboratory for Magnetism and Magnetic Materials of MOE, Lanzhou University, Lanzhou, Gansu 730000, China*

[2]*Department of Physics and Astronomy and National Superconducting Cyclotron Laboratory Michigan State University, East Lansing, Michigan 48824-1321, USA*

[3]*Institut für Kernphysik, Technische Universität Darmstadt, D-64289 Darmstadt, Germany*

(Received 15 May 2018; revised manuscript received 18 July 2018; published 20 November 2018)

Recent high-resolution nuclear resonance fluorescence experiments performed on the even-even Chromium isotopes ^{50,52,54}Cr have lead to the identification (energy, spin, parity, and transition strength) of altogether 108 nuclear levels of spin $J = 1$ (70 levels with $J^\pi = 1^-$ and 38 with $J^\pi = 1^+$) at excitation energies E_x ranging roughly from 4.5 to 9.7 MeV. In this region just above the orbital magnetic-dipole scissors mode, sizable spin-flip magnetic-dipole strength as well as electric-dipole strength belonging to the pygmy dipole resonance (PDR) is expected. Using statistical measures for short- and long-range correlations, we perform an analysis of the fluctuation properties in the subspectra of the energy levels and also of the distributions of their respective dipole transition strengths. We compare the results with those of a random matrix ensemble interpolating between Poisson statistics generally describing the fluctuation properties in the energy spectra of many-body systems with collective, i.e., regular motion of the particles and the Gaussian orthogonal ensemble (GOE) for complex (i.e., chaotic) behavior. This comparison reveals that the spectral properties of the 1^+ states are close to the GOE results while those of the 1^- states are closer to Poisson. This is confirmed by an analysis of the spectral fluctuations based on the method of Bayesian inference and corroborated by large-scale shell-model and quasiparticle-phonon model calculations, respectively. The nearly Poissonian behavior of the 1^- levels suggests a sizable collectivity of the PDR indeed.

DOI: 10.1103/PhysRevC.98.054314

I. INTRODUCTION

Rich information on nuclear structure from recent high-resolution nuclear resonance fluorescence experiments [1–3] on the three stable isotopes ^{50,52,54}Cr with proton number $Z = 24$ and neutron numbers $N = 26$, 28, and 30, respectively, affords an excellent opportunity to investigate spectral fluctuation properties of complex many-body systems in the realm of quantum chaos. The data consist of excitation energies of $J^\pi = 1^-$ and 1^+ states and of the respective electric $B(E1)$ and magnetic $B(M1)$ dipole transition strengths. For ^{52}Cr the data were obtained at the Superconducting Darmstadt Electron Linear Accelerator (S-DALINAC) and have already been published in Ref. [1] while those for ^{50,54}Cr stem from recent measurements [2,3] at the S-DALINAC and the high-intensity γ-ray source (HIγS) of the Triangle Universities Nuclear Laboratory (TUNL). Some experimental details relevant for the particular analysis discussed in the present article are given in Table I. As listed there, dipole excitations were observed at excitation energies from as low as 4.5 MeV up to 9.7 MeV. In this region, just above the scissors mode, which consists of orbital $M1$ strength, sizable spin-flip $M1$ strength from $1f_{7/2} \rightarrow 1f_{5/2}$ and $2p_{3/2} \rightarrow 2p_{1/2}$ shell-model excitations is expected [4]. This is, however, also the region of low-energy $E1$ strength commonly termed the pygmy dipole resonance (PDR) [5].

Figures 1 and 2 present the experimental $B(E1)$ and $B(M1)$ transition strengths for ^{50,52,54}Cr together with quasiparticle-phonon and shell-model calculations to be discussed below. It is *not* the aim to enter into a thorough discussions of the underlying nuclear structure of the particular $M1$ and $E1$ excitations observed, for which predictions from a whole variety of nuclear models exist—often with conflicting conclusions, in particular for the interpretation of the PDR. We rather suggest following an alternative approach based on random matrix theory (RMT) which allows us to analyze the spectral properties of the excited $J^\pi = 1^-$ and 1^+ states within the same region of excitation energy to draw conclusions about their single-particle or collective character. Furthermore, this approach renders possible the comparison of the experimental data with those obtained from large-scale shell-model and quasiparticle-phonon model calculations. To our knowledge, this particular RMT analysis has not been done before and reveals interesting results with respect to the nature of the PDR. Briefly, the fluctuation properties in the spectra of generic quantum systems with classically integrable

*Dietz@lzu.edu.cn
†brown@nscl.msu.edu
‡Pietralla@ikp.tu-darmstadt.de
§ponomare@theorie.ikp.physik.tu-darmstadt.de
‖Richter@ikp.tu-darmstadt.de

TABLE I. The number of energy levels N with spin $J = 1$ and positive ($\pi = +$), respectively, negative ($\pi = -$) parity, measured in ^{50}Cr, ^{52}Cr, and ^{54}Cr, the corresponding energy ranges and the smallest experimentally observed transition strength $B_{\min}$.

Nucleus	Parity	N	Energy range	$B_{\min}$
^{50}Cr	$-$	17	6.3–9.4 MeV	0.00046 e^2 fm^2
^{50}Cr	$+$	12	7.6–9.7 MeV	0.04500 μ_n^2
^{52}Cr	$-$	16	6.4–9.2 MeV	0.00050 e^2 fm^2
^{52}Cr	$+$	9	6.8–9.4 MeV	0.03800 μ_n^2
^{54}Cr	$-$	37	6.6–9.7 MeV	0.00076 e^2 fm^2
^{54}Cr	$+$	17	4.5–9.6 MeV	0.00059 μ_n^2

dynamics are predicted to coincide with those of Poissonian random numbers [6]. In contrast, those of time-reversal invariant chaotic systems generally coincide with the spectral properties of the eigenvalues of real-symmetric matrices with Gaussian distributed random entries from the Gaussian orthogonal ensemble (GOE) [7–12], in accordance with the Bohigas–Giannoni–Schmit conjecture [13]. Similar features are observed in the energy spectra of nuclear many-particle systems even though there is no obvious classical analog [14–16]. If the motion of the nucleons is collective, their spectral properties coincide with those of random Poissonian numbers, whereas they are well described by the GOE if it is sufficiently complex [16–19]. There are various semiclassical [20–23] and RMT approaches [16,24–26] to obtain information on the chaoticity vs regularity in a nuclear many-body system. We analyzed spectral fluctuation properties of ^{50,52,54}Cr by proceeding similarly to Ref. [27], and the distributions of the transition strengths by following Ref. [28].

II. ANALYSIS OF THE EXPERIMENTAL DATA

First, we present results on the fluctuation properties in the energy spectra of the low-lying electric ($E1$) and magnetic ($M1$) dipole excitations in the nuclei ^{50}Cr, ^{52}Cr,

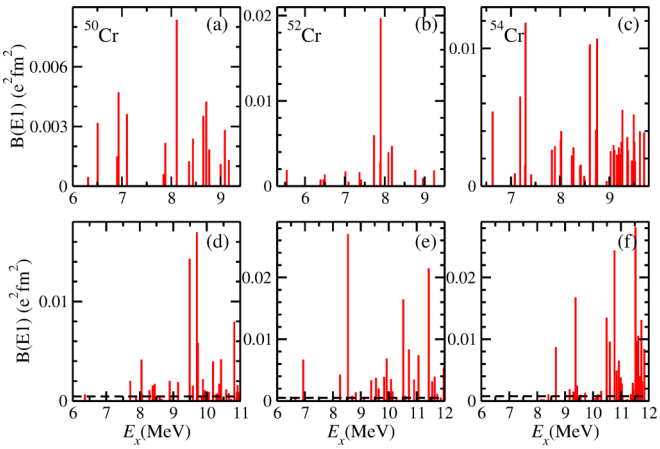

FIG. 1. Transition strength $B(E1)$ for the 1^- states. (a)–(c) Experimentally determined strengths [1–3]. (d)–(f) Calculated strengths as described in the main text. The black dashed lines indicate the experimental threshold for detectability.

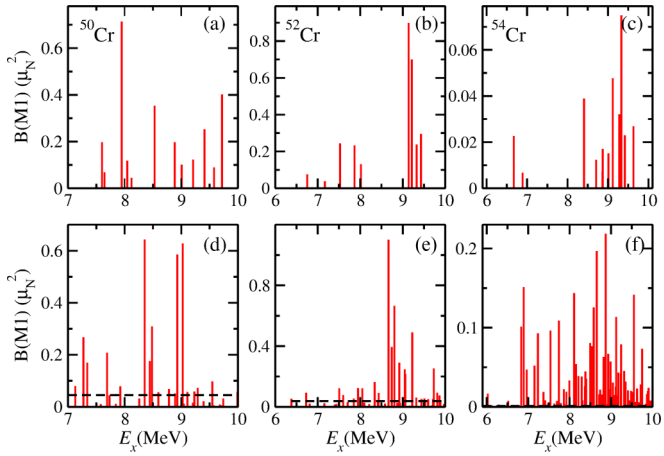

FIG. 2. Transition strength $B(M1)$ for the 1^+ states. (a)–(c) Experimentally determined strengths [1–3]. (d)–(f) Calculated strengths as described in the main text. The black dashed lines indicate the experimental threshold for detectability.

and ^{54}Cr corresponding to angular momentum $J = 1$ with negative ($\pi = -$) and positive ($\pi = +$) parity, respectively. The numbers of observed excitations and the energy ranges are listed in Table I. To obtain information on the chaoticity of these nuclear many-body systems we evaluated for each sequence separately [29] the nearest-neighbor spacing distribution (NNSD) $P(s)$, the number variance Σ^2, the Dyson–Mehta Δ_3 statistics [10–12] which provides the least-square deviation of the integrated spectral density from the best-fit straight line, the distribution $P(r)$ of the ratios of consecutive level spacings [26,30,31], and the distributions of the transition strengths $B(E1)$ and $B(M1)$ [28]. Since the spacing ratios are dimensionless, no unfolding of the energy levels is needed for the determination of $P(r)$. This can be of great advantage, especially when no analytical expression for the smooth part of the integrated spectral density is available.

The energy levels E_i in each sequence were unfolded by replacing them by the smooth part $e_i = \bar{N}(E_i)$ of the integrated spectral density, yielding a mean spacing of unity, $\langle s \rangle = 1$. For this we fit an empirical formula [32,33], $\bar{N}(E) = \exp[(E - E_0)/T] + N_0$ with T, E_0, and N_0 being the fit parameters to $\bar{N}(E_i)$. It was applied hitherto to low-lying nuclear levels in Ref. [34].

In Figs. 3(a) and 3(b) we show the resulting NNSD (histograms) for the negative and positive parity states, respectively, in ^{54}Cr. Both are compared with the NNSD of Poissonian random numbers (dashed lines) and of eigenvalues drawn from the GOE (full lines). While the 1^+ states exhibit a behavior which is close to GOE, the NNSD of the 1^- states is closer to Poisson. To scrutinize these results, we also computed the statistical measures for the other two nuclei (see Figs. 4 and 5) and then performed ensemble averages, separately, for the positive- and negative-parity states. The results are summarized in Figs. 6 and 7, respectively. Although we are dealing with three nuclei of different structure—^{50}Cr has two holes in the $N = 28$ shell, ^{52}Cr is semimagic, and ^{54}Cr has two neutrons above the closed shell—their statistical properties are similar.

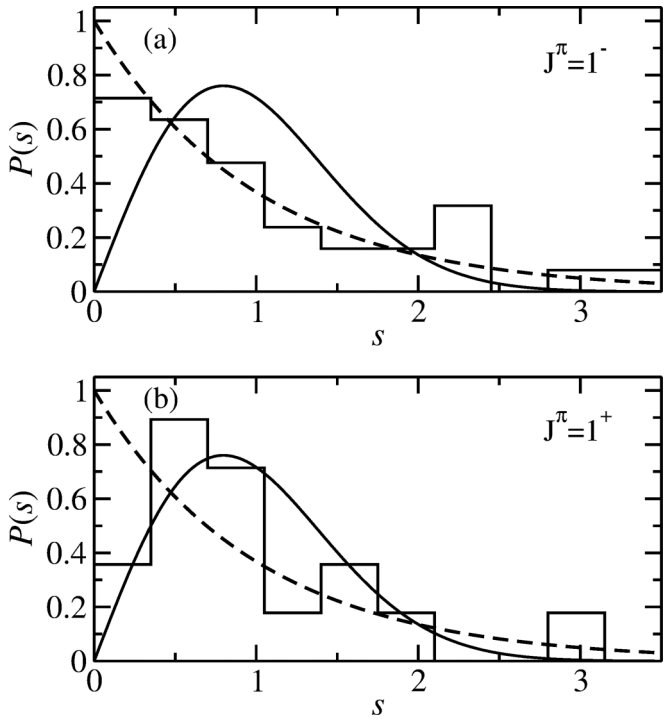

FIG. 3. Nearest-neighbor spacing distributions of the experimental (a) $J^\pi = 1^-$ and (b) $J^\pi = 1^+$ energy levels of ^{54}Cr (histograms) in comparison with the Poisson (dashed lines) and the GOE (full line) results.

Deviations of Σ^2 from GOE for $L \gtrsim 1$ in Fig. 6 and from Poisson in Fig. 7 may be attributed to the short lengths of the level sequences (see Table I). Another possible explanation might be the incompleteness of the spectra. Analytical expressions were derived for such spectra on the basis of the results for the Gaussian ensembles of random matrices in Ref. [35]. The NNSD of a system exhibiting GOE behavior in the complete spectrum is expressed in terms of a sum over the $(n+1)$st nearest-neighbor spacing distributions of the GOE with $n = 1, 2, \ldots$, which depend on s/φ instead of the spacing s, with φ denoting the fraction of detected levels. Similarly, the Σ^2 and Δ_3 statistics are given in terms of the corresponding GOE results with the argument depending on φ. This missing level statistics describes well the statistical measures obtained for the 1^+ states for values of φ corresponding to 30% of missing levels for ^{50}Cr and ^{52}Cr and 16% for ^{54}Cr (see Fig. 8). Such a good agreement was not found for the spectral properties of the 1^- states. Their comparison with missing level statistics yielded $\varphi = 0.4$ (see Fig. 8), which would imply 60% of missing levels. We, furthermore, compared the spectral properties of the 1^+ and 1^- states to those of a random matrix ensemble interpolating between Poisson for $\lambda = 0$ and GOE for $\lambda = 1$ (see Refs. [25,27,36,37]) yielding $\lambda = 0.8$ and $\lambda = 0.3$, respectively (see Fig. 9), thus indicating that the behavior of the 1^- states indeed is close to Poisson, whereas it is close to GOE for the 1^+ states. At this point we would like to emphasize that the Poissonian statistics does not originate from weakly interacting $1p-1h$ and $3p-3h$ states. Actually,

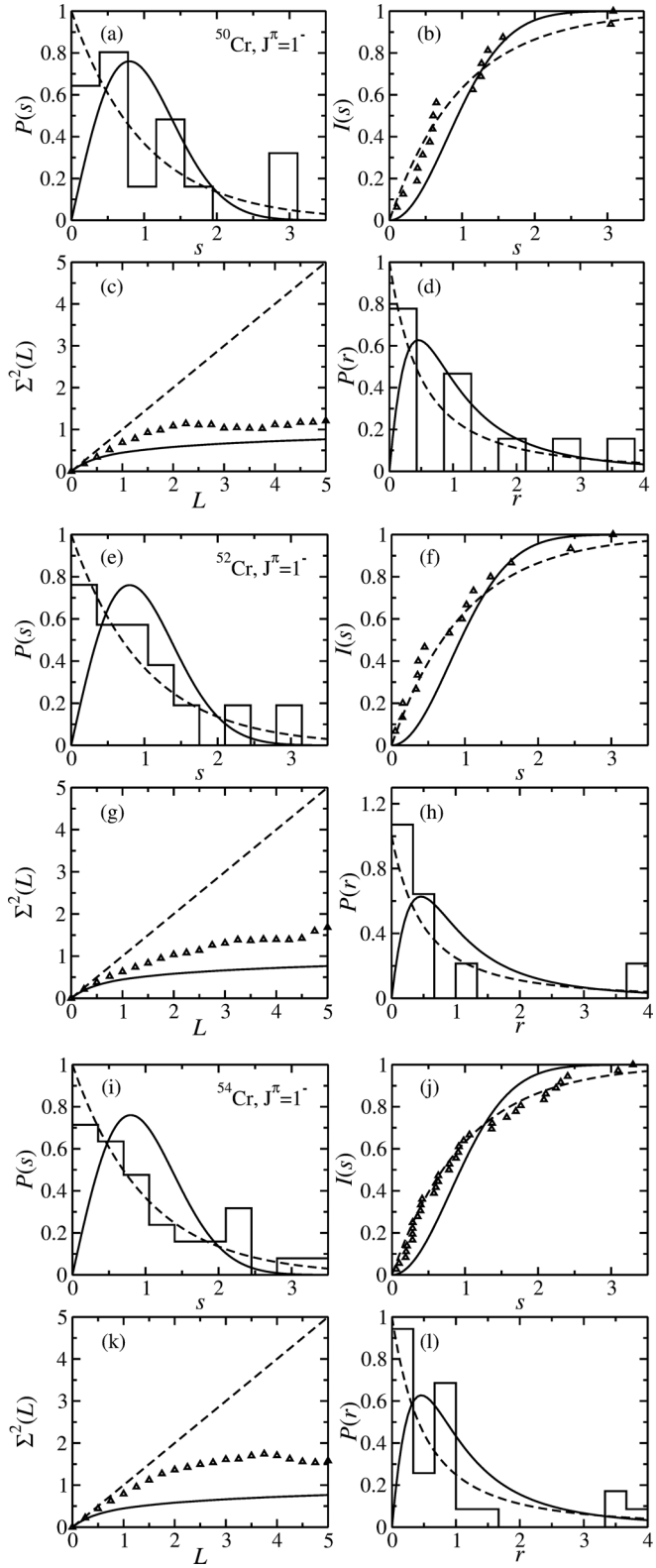

FIG. 4. Spectral statistics of the experimental 1^- energy levels of ^{50}Cr, ^{52}Cr, and ^{54}C (up-triangles and histograms) as indicated in the insets in comparison to the Poissonian (dashed lines) and the GOE (full lines) results. Shown are the nearest-neighbor spacing distribution $P(s)$, the integrated nearest-neighbor spacing distribution $I(s)$, the number variance $\Sigma^2(L)$, and the ratio distribution $P(r)$.

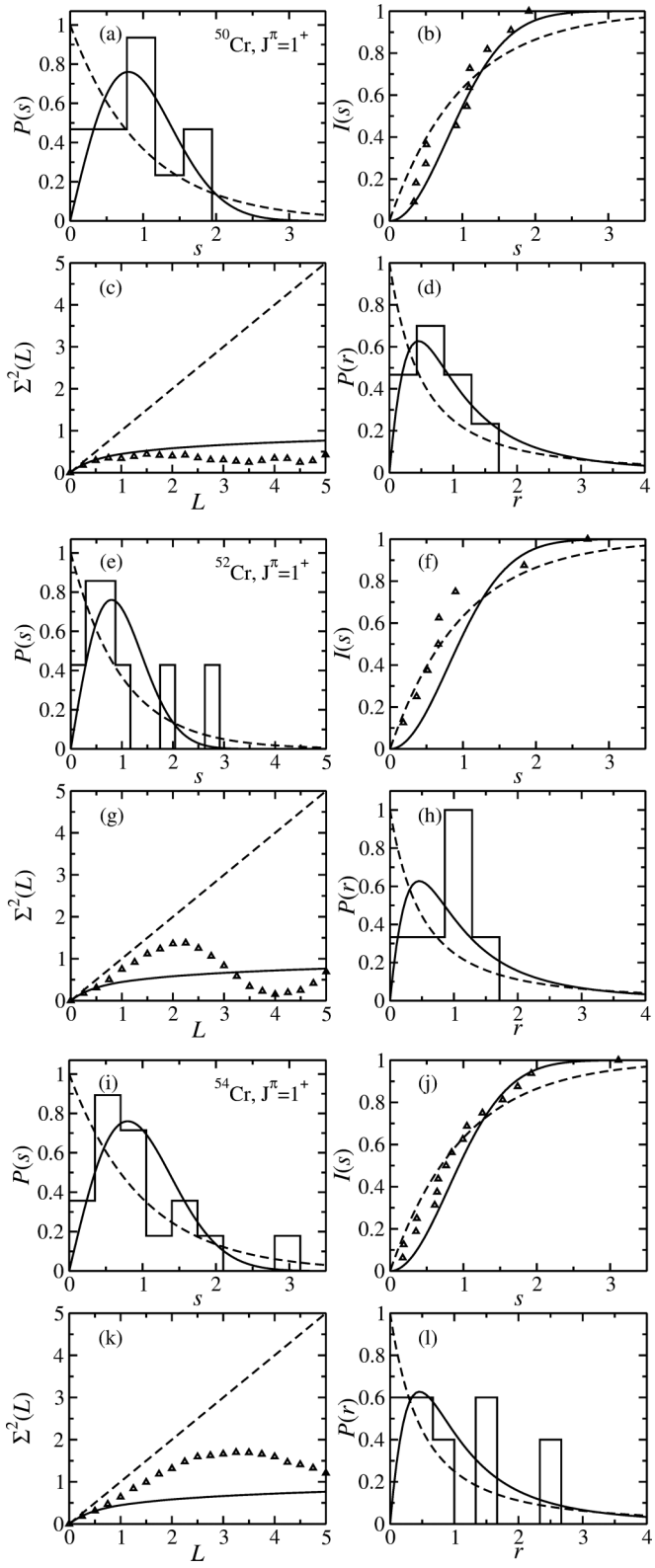

FIG. 5. Same as Fig. 4 for the experimental 1^+ energy levels of ^{50}Cr, ^{52}Cr, and ^{54}C as indicated in the insets.

the excitation of $3p-3h$ states from the nuclear ground state through photon scattering is of higher order and therefore not

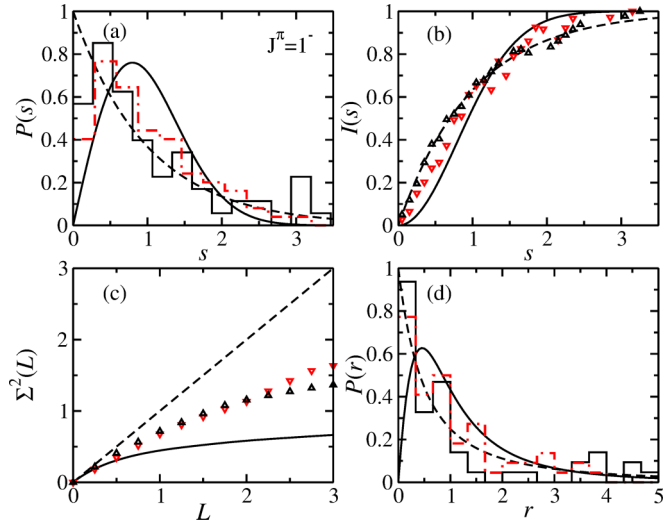

FIG. 6. Comparison of the averaged spectral fluctuation properties of the experimental $J^\pi = 1^-$ energy levels of ^{50}Cr, ^{52}Cr, and ^{54}Cr with the Poisson (dashed lines) and the GOE (full lines) results and those obtained from QPM calculations (red down-triangles and dash-dotted lines).

observed in our experimental spectra. Accordingly, $3p-3h$ states are not included in the theoretical analysis.

To further validate this assumption, we followed an idea of Rosenzweig and Porter [38], and considered superimposed spectra of positive and negative parity, respectively, composed of those of ^{50}Cr, ^{52}Cr, and ^{54}Cr. We analyzed their fluctuation properties in terms of the NNSD using the method of Bayesian inference [39] which involves a chaoticity parameter $\bar{f}$ interpolating between Poisson ($\bar{f} = 0$) and GOE statistics ($\bar{f} = 1$). For this, we first computed the spacings between adjacent unfolded energy levels for each nucleus separately, and then merged them according to the associated parity into

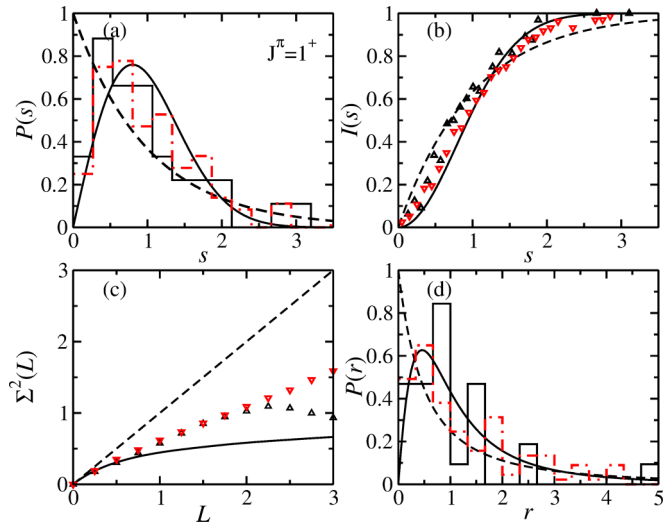

FIG. 7. Same as Fig. 6. Comparison of the results for the experimental $J^\pi = 1^+$ energy levels with those obtained from shell-model calculations (red down-triangles and dash-dotted lines).

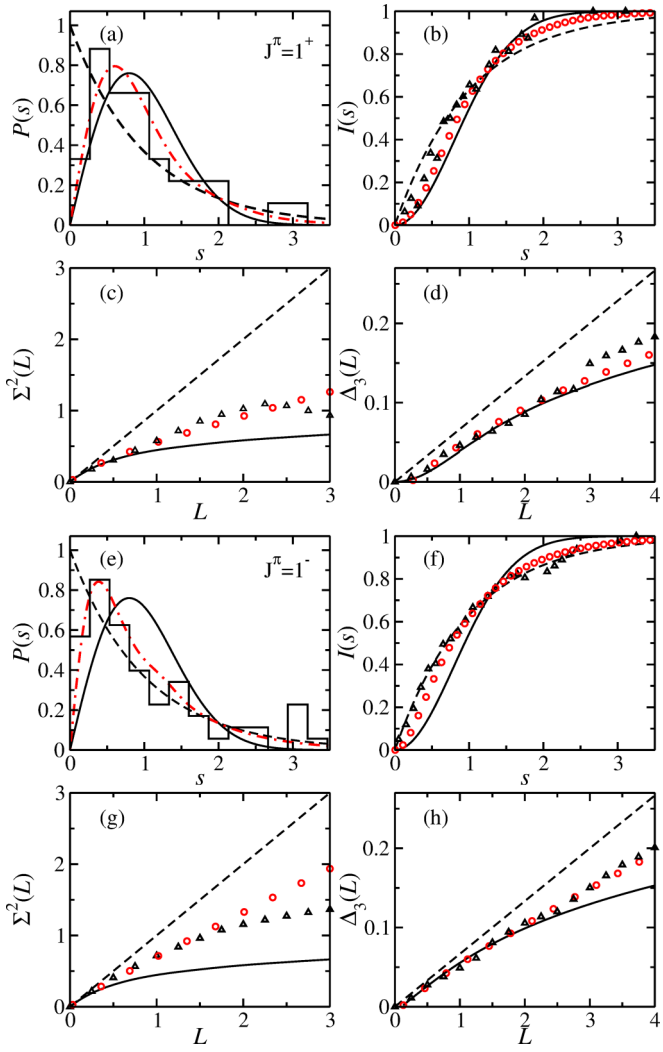

FIG. 8. Comparison of the averaged spectral fluctuation properties of the experimental 1^+ and 1^- energy levels of ^{50}Cr, ^{52}Cr, and ^{54}Cr with the Poisson (dashed lines) and the GOE (full lines) results and with those obtained from missing-level statistics [35] (red circles and dash-dotted lines). Best agreement was found for a fraction of $\varphi = 0.75$ detected ones, corresponding to 25% for the 1^+ states and $\varphi = 0.4$ corresponding to 60% missing levels for the 1^- states.

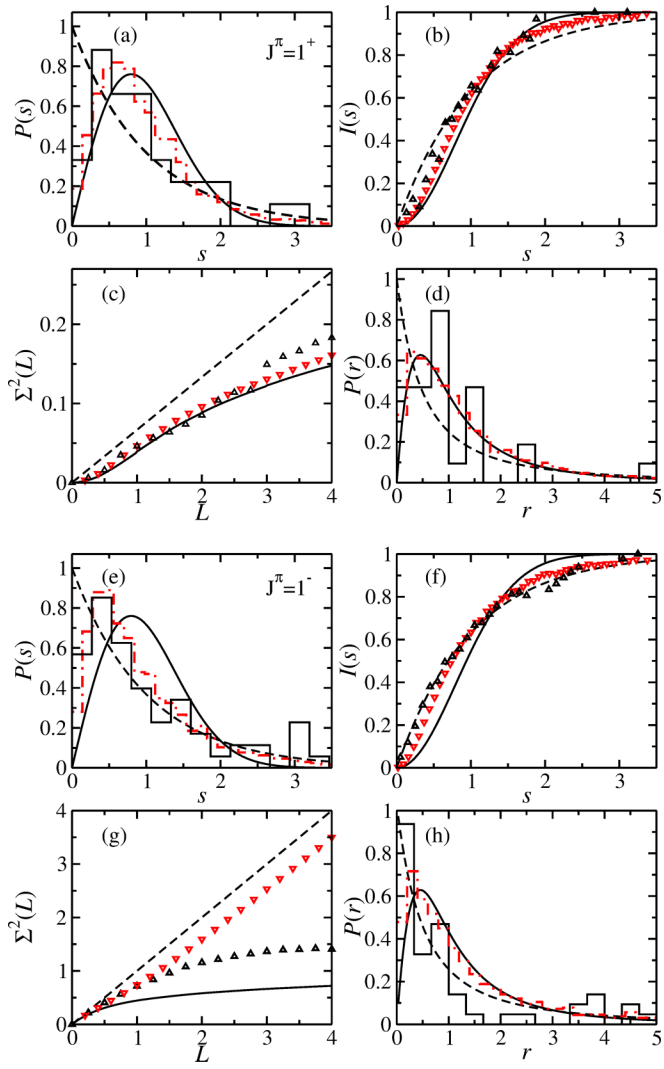

FIG. 9. Same as Fig. 8. Comparison with the spectral statistics of a random matrix ensemble interpolating between Poisson ($\lambda = 0$) and GOE [25,27,36,37] ($\lambda = 1$) (red down triangles and dash-dotted lines). Best agreement was found for $\lambda = 0.8$ for the 1^+ states and $\lambda = 0.3$ for the 1^- states.

two sequences of spacings [40–42]. For the determination of the parameter $\bar{f}$ we proceeded as described in Ref. [27]. The resulting NNSDs for negative and positive parity are shown in Figs. 10(a) and 10(b), respectively.

Besides the spectral fluctuation properties we also analyzed the distributions of the transition strengths $B(E1)$ and $B(M1)$. For this we proceeded as described in Ref. [28]. Accordingly, we first unfolded the measured transition strengths B_i for each nucleus and parity, i.e., for $B_i = B(E1)$ and $B_i = B(M1)$, individually by dividing them by an average value, $y_i = B_i/B_{av,i}$, with $B_{av,i} = \sum_j B_j \exp[-(e_i - e_j)^2/8]/\sum_j \exp[-(e_i - e_j)^2/8]$ denoting the average around the transition strength B_i. The ensemble-averaged distributions of y_i are shown in Figs. 11(a) and 11(b) (full-line histograms) for negative and positive parities, respectively. Figures 11(c) and 11(d) show the distributions of $z_i = \log_{10}(y_i)$. The results are compared with a truncated Porter–Thomas distribution, which is obtained by considering only values of $y \geqslant y_0$, where y_0 denotes the minimal observed transition strength. The agreement is good for the 1^+ states whereas the deviations from Porter–Thomas behavior observed for the 1^- states may be attributed to a nearly Poissonian behavior [28] in accordance with the spectral fluctuation properties exhibited by the corresponding energy levels.

III. ANALYSIS OF SPECTRA FROM NUCLEAR MODEL CALCULATIONS

The results for the fluctuation properties of the energy levels and transition strengths were also compared with model calculations. We performed shell-model calculations by employing effective KB3G and GPFX1A interactions for the

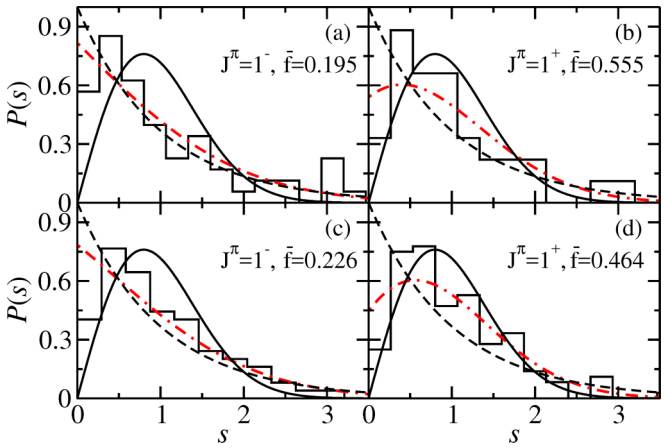

FIG. 10. Nearest-neighbor spacing distribution of the experimental energy levels with (a) $J^\pi = 1^-$ and (b) $J^\pi = 1^+$ in comparison with the NNSDs of the calculated ones for (c) $J^\pi = 1^-$ and (d) $J^\pi = 1^+$ obtained by taking into account only those levels with transition strengths above the experimental minimum value. They are compared with the Poisson (dashed line) and the GOE (full line) distributions. The dash-dotted curves in red were determined with the method of Bayesian inference. The resulting values for the chaoticity parameter $\bar{f}$ are given in the insets.

description of the spectral properties of the $J^\pi = 1^+$ states and quasiparticle-phonon model (QPM) calculations for the $J^\pi = 1^-$ states. The calculated individual transition strengths are shown in Figs. 1 and 2 and are compared there to the respective experimental ones. The center of gravity is about 1 MeV lower than the experimental one for the 1^+ states while it is roughly 2 MeV higher for the 1^- states.

Excitation energies and $B(M1)$ values for the 1^+ states were obtained from configuration-interaction calculations in

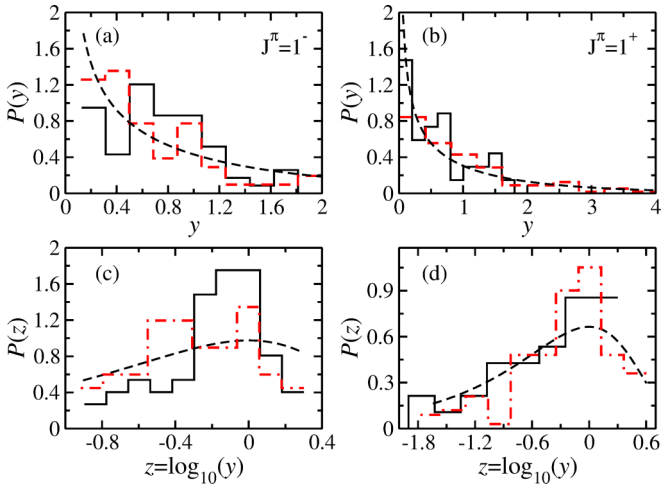

FIG. 11. (a), (b) Averaged distribution of the unfolded transition strengths $y_i = B_i/B_{av,i}$ and of (c), (d) $z_i = \log_{10}(y_i)$ of the experimental results (histograms) for the (a), (c) $J^\pi = 1^-$ and (b), (d) $J^\pi = 1^+$ states in comparison with a truncated Porter–Thomas distribution $P(y)$ with $y \geqslant y_0$ and y_0 denoting the smallest experimentally observed transition strength (dashed and dash-dotted lines).

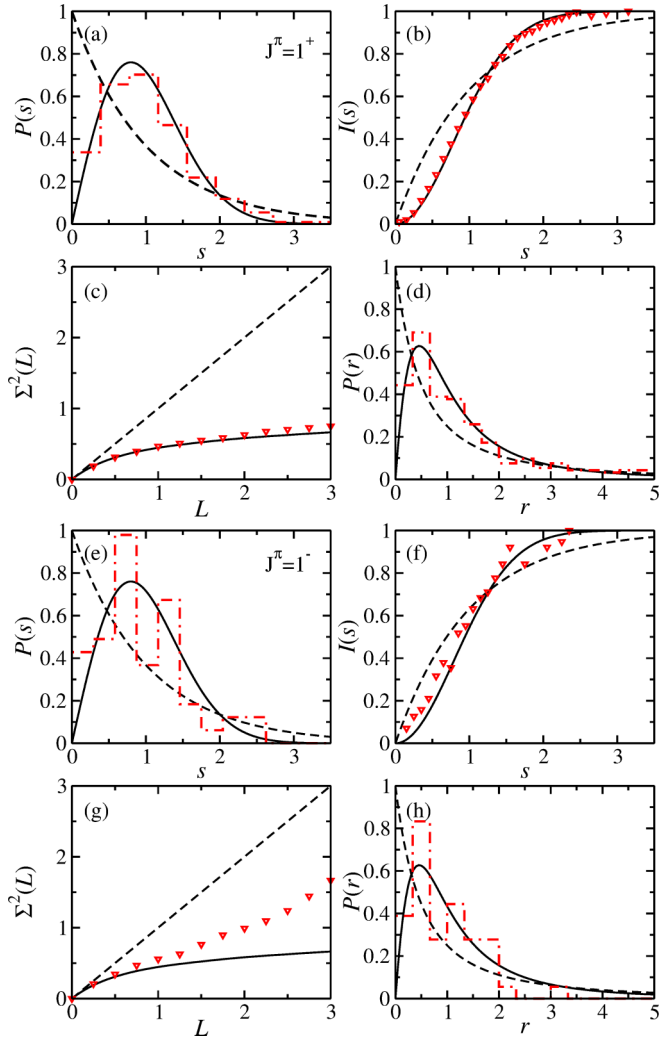

FIG. 12. Averaged spectral statistics of the 1^+ and 1^- energy levels obtained from shell-model calculations using the effective KB3G interaction and from QPM calculations (red dash-dotted lines and histograms), respectively. Here, the number of energy levels taken into account for each nucleus was chosen to be similar to those of the corresponding experimental energy levels.

the pf model space with the shell-model code NUSHELLX [43] employing the effective Hamiltonians KB3G [44] and GPFX1A [45]. The $B(M1)$ values were reduced by a factor of 0.5 to take into account the quenching of observed $M1$ strength in ^{48}Ca compared with these types of calculation [46]. Excitation energies and $B(E1)$ values for the 1^- states were calculated based on the QPM [47] employing the Woods–Saxon potential with parameters from global parametrization as a mean field. All single-particle levels from the bottom up to narrow quasibound levels in the continuum are accounted for. To describe excited states of nuclei, the model Hamiltonian is diagonalized in two steps. First, the $1p-1h$ excitations are projected on quasibosonic 1-phonon configurations of different multipolarity by solving equations of the quasiparticle random-phase approximation with the residual interaction in separable form. Then, excited states are described by wave functions made up of interacting

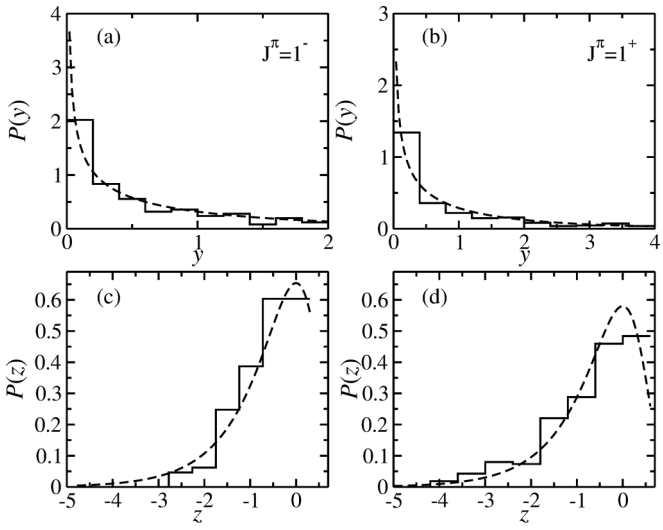

FIG. 13. (a), (b) Averaged distribution of the unfolded transition strengths $y_i = B_i/B_{av,i}$ and (c), (d) $z_i = \log_{10}(y_i)$ obtained from QPM and shell-model calculations including the KB3G interaction (histograms) for the (a), (c) $J^\pi = 1^-$ and (b), (d) $J^\pi = 1^+$ states, respectively, in comparison with the Porter–Thomas distribution (dashed lines).

one- and multiphonon configurations. Their energies and internal fermion structure are obtained by the second diagonalization of the model Hamiltonian on the set of these states. For details, see Refs. [48,49]. In the calculations presented below, the basis contains phonons of multipolarities from $1^\pm$ to $7^\pm$. Only two-phonon configurations with excitation energies below 20 MeV have been taken into account.

The results for the spectral fluctuation properties and the distributions of the transition strengths are shown in Figs. 12 and 13. Here, the numbers of levels taken into account were chosen similar to those of the experimental levels. For the 1^+ case the agreement with GOE is very good, while for the 1^- states small deviations towards Poisson are observed. For the description of the experimental data in each sequence of calculated levels only those were taken into account for which the transition strength was larger or equal to the smallest experimentally observed ones. For the 1^+ states the number of the thus removed energy levels was similar to that of the missing levels estimated based on the missing-level statistics for the experimental ones. In the case of the 1^- states, smaller fractions of energy levels needed to be removed [50]. This corroborates our assumption that the deviations of the spectral properties of the corresponding experimental data may not be attributed to a large number of missing levels, but are indeed Poissonian like. The results deduced from the model calculations are shown in Figs. 6–10.

IV. CONCLUSION

We have investigated the fluctuation properties in the energy spectra of $J^\pi = 1^-$ and $J^\pi = 1^+$ states in the three medium-heavy nuclei ^{50,52,54}Cr between about 4.5 and 9.7 MeV within the RMT approach. The results for the 1^+ states show evidence for correlations between the unfolded levels which are similar to GOE behavior. The situation is different for the 1^- states which lack level correlations and, thus, behave like Poissonian random numbers. These findings are corroborated by large-scale shell-model and quasiparticle-phonon model calculations, respectively. The dominantly regular behavior of the 1^- states is consistent with an interpretation of the PDR within an extreme semiclassical picture in which the excess neutrons forming a skin around a core oscillate collectively in dipole-like motion against the latter [5]. In passing we note further that the method of using RMT to draw this conclusion has also been successfully applied before to the fine structure of orbital magnetic-dipole excitations belonging to the scissors mode [51]. The corresponding semiclassical picture is the rotational motion of two ellipsoids of all neutrons and protons, respectively, performing small-angle oscillations against each other [4].

ACKNOWLEDGMENTS

This work was supported by the Deutsche Forschungsgemeinschaft (DFG) within the Collaborative Research Center 1245. B.A.B. acknowledges U.S. NSF Grant No. PHY-1811855. B.D. thanks the National Natural Science Foundation of China for financial support under Grant No. 11775100.

[1] H. Pai, J. Beller, N. Benouaret, J. Enders, T. Hartmann, O. Karg, P. von Neumann-Cosel, N. Pietralla, V. Yu. Ponomarev, C. Romig, M. Scheck, L. Schnorrenberger, S. Volz, and M. Zweidinger, Phys. Rev. C **88**, 054316 (2013).
[2] H. Pai, T. Beck, J. Beller, R. Beyer, M. Bhike, V. Derya, U. Gayer, J. Isaak, Krishichayan, J. Kvasil, B. Löher, V. O. Nesterenko, N. Pietralla, G. Martínez-Pinedo, L. Mertes, V. Yu. Ponomarev, P.-G. Reinhard, A. Repko, P. C. Ries, C. Romig, D. Savran, R. Schwengner, W. Tornow, V. Werner, J. Wilhelmy, A. Zilges, and M. Zweidinger, Phys. Rev. C **93**, 014318 (2016).
[3] P. C. Ries, H. Pai, T. Beck, J. Beller, M. Bhike, U. Gayer, J. Isaak, B. Löher, Krishidhaoan, L. Mertes, N. Pietralla, V. Yu. Ponomarev, C. Romig, D. Savran, M. Schilling, W. Tornow, V. Werner, and M. Zweidinger (unpublished).
[4] K. Heyde, P. von Neumann-Cosel, and A. Richter, Rev. Mod. Phys. **82**, 2365 (2010).
[5] D. Savran, T. Aumann, and A. Zilges, Prog. Part. Nucl. Phys. **70**, 210 (2013).
[6] M. V. Berry and M. Tabor, Proc. R. Soc. London, Ser. A **356**, 375 (1977).
[7] S. W. McDonald and A. N. Kaufman, Phys. Rev. Lett. **42**, 1189 (1979).
[8] G. Casati, F. Valz-Gris, and I. Guarneri, Lett. Nuovo Cimento **28**, 279 (1980).
[9] M. V. Berry, Eur. J. Phys. **2**, 91 (1981).
[10] F. J. Dyson and M. L. Mehta, J. Math. Phys. **4**, 701 (1963).
[11] M. L. Mehta, *Random Matrices* (Academic Press, London, 1990).

[12] O. Bohigas and M. J. Giannoni, Ann. Phys. (NY) **89**, 393 (1975).

[13] O. Bohigas, M. J. Giannoni, and C. Schmit, Phys. Rev. Lett. **52**, 1 (1984).

[14] T. A. Brody, J. Flores, J. B. French, P. A. Mello, A. Pandey, and S. S. M. Wong, Rev. Mod. Phys. **53**, 385 (1981).

[15] T. Guhr, A. Müller-Groeling, and H. A. Weidenmüller, Phys. Rep. **299**, 189 (1998).

[16] J. M. G. Gómez, K. Kar, V. K. B. Kota, R. A. Molina, A. Relaño, and J. Retamosa, Phys. Rep. **499**, 103 (2011).

[17] T. Guhr and H. A. Weidenmüller, Ann. Phys. (NY) **193**, 472 (1989).

[18] V. V. Flambaum, A. A. Gribakina, G. F. Gribakin, and M. G. Kozlov, Phys. Rev. A **50**, 267 (1994).

[19] V. Zelevinsky, B. A. Brown, N. Frazier, and M. Horoi, Phys. Rep. **276**, 85 (1996).

[20] J. Hämmerling, B. Gutkin, and T. Guhr, J. Phys. A: Math. Theor. **43**, 265101 (2010).

[21] T. Engl, J. D. Urbina, and K. Richter, Phys. Rev. E **92**, 062907 (2015).

[22] R. Dubertrand and S. Müller, New J. Phys. **18**, 033009 (2016).

[23] M. Akila, D. Waltner, B. Gutkin, P. Braun, and T. Guhr, Phys. Rev. Lett. **118**, 164101 (2017).

[24] H. A. Weidenmüller and G. E. Mitchell, Rev. Mod. Phys. **81**, 539 (2009).

[25] V. K. B. Kota, *Lecture Notes in Physics* (Springer, Heidelberg, 2014), Vol. 884.

[26] V. K. B. Kota and N. D. Chavda, Int. J. Mod. Phys. E **27**, 1830001 (2018).

[27] B. Dietz, A. Heusler, K. H. Maier, A. Richter, and B. A. Brown, Phys. Rev. Lett. **118**, 012501 (2017).

[28] J. Enders, T. Guhr, A. Heine, P. von Neumann-Cosel, V. Yu. Ponomarev, A. Richter, and J. Wambach, Nucl. Phys. A **741**, 3 (2004).

[29] O. Bohigas, R. U. Haq, and A. Pandey, in *Nuclear Data for Science and Technology*, edited by K. H. Böckhoff (Reidel, Dordrecht, 1983).

[30] Y. Y. Atas, E. Bogomolny, O. Giraud, and G. Roux, Phys. Rev. Lett. **110**, 084101 (2013).

[31] B. Dietz, T. Klaus, M. Miski-Oglu, A. Richter, M. Wunderle, and C. Bouazza, Phys. Rev. Lett. **116**, 023901 (2016).

[32] A. G. W. Cameron and R. M. Elkin, Can. J. Phys. **43**, 1288 (1965).

[33] A. Gilbert and A. G. W. Cameron, Can. J. Phys. **43**, 1446 (1965).

[34] J. F. Shriner, Jr., G. E. Mitchell, and T. von Egidy, Z. Phys. A: Hadrons Nucl. **338**, 309 (1991).

[35] O. Bohigas and M. P. Pato, Phys. Lett. B **595**, 171 (2004).

[36] G. Lenz and F. Haake, Phys. Rev. Lett. **67**, 1 (1991).

[37] H. Alt, H.-D. Gräf, H. L. Harney, R. Hofferbert, H. Lengeler, C. Rangacharyulu, A. Richter, and P. Schardt, Phys. Rev. E **50**, R1(R) (1994).

[38] N. Rosenzweig and C. E. Porter, Phys. Rev. **120**, 1698 (1960).

[39] H. L. Harney, *Bayesian Inference—Parameter Estimation and Decisions* (Springer, Heidelberg, 2003).

[40] A. Y. Abul-Magd and M. H. Simbel, Phys. Rev. C **54**, 1675 (1996).

[41] A. Y. Abul-Magd, H. L. Harney, M. H. Simbel, and H. A. Weidenmüller, Phys. Lett. B **579**, 278 (2004).

[42] A. Y. Abul-Magd, H. L. Harney, M. H. Simbel, and H. A. Weidenmüller, Ann. Phys. (NY) **321**, 560 (2006).

[43] B. A. Brown and W. D. M. Rae, Nucl. Data Sheets **120**, 115 (2014).

[44] A. Poves, J. Sanchez-Solano, E. Caurier, and F. Nowacki, Nucl. Phys. A **694**, 157 (2001).

[45] M. Honma, T. Otsuka, B. A. Brown, and T. Mizusaki, Eur. Phys. J. A **25** Suppl. 1, 499 (2005).

[46] M. Mathy, J. Birkhan, H. Matsubara, P. von Neumann-Cosel, N. Pietralla, V. Yu. Ponomarev, A. Richter, and A. Tamii, Phys. Rev. C **95**, 054316 (2017).

[47] V. G. Soloviev, *Theory of Atomic Nuclei, Quasiparticles and Phonons* (IOP, London, 1982).

[48] C. A. Bertulani and V. Yu. Ponomarev, Phys. Rep. **321**, 139 (1999).

[49] N. Lo Iudice, V. Yu. Ponomarev, Ch. Stoyanov, A. V. Sushkov, and V. V. Voronov, J. Phys. G **39**, 043101 (2012).

[50] Adding three-phonon configurations which have $B(E1) = 0$ and are out of the model space in the present QPM calculations brings the number of weakly excited 1^- states close to the 60% of missing levels obtained from the statistical analysis of the data.

[51] J. Enders, T. Guhr, N. Huxel, P. von Neumann-Cosel, C. Rangacharyulu, and A. Richter, Phys. Lett. B **486**, 273 (2000).